Tectonics

RESEARCH ARTICLE
10.1029/2019TC005810

Key Points:
- Detrital zircons with North American basement ages are spatiotemporally ubiquitous in the stratigraphy of western North America
- Ubiquity is due to orogenic recycling of detrital zircons through multiple phases of basin evolution
- The presence of North American basement ages alone does not identify unique sediment source areas

Supporting Information:
- Supporting Information S1
- Figure S1
- Table S1

Correspondence to:
T. M. Schwartz,
tmschwartz@usgs.gov

Citation:
Schwartz, T. M., Schwartz, R. K., & Weislogel, A. L. (2019). Orogenic recycling of detrital zircons characterizes age distributions of North American Cordilleran strata. *Tectonics*, *38*, 4320–4334. https://doi.org/10.1029/2019TC005810

Received 6 AUG 2019
Accepted 26 NOV 2019
Accepted article online 28 NOV 2019
Published online 17 DEC 2019

Orogenic Recycling of Detrital Zircons Characterizes Age Distributions of North American Cordilleran Strata

T.M. Schwartz[1], **R.K. Schwartz**[2], **and A.L. Weislogel**[3]

[1]Geosciences and Environmental Change Science Center, U.S. Geological Survey, Denver, CO, USA, [2]Department of Geology, Allegheny College, Meadville, PA, USA, [3]Department of Geology and Geography, West Virginia University, Morgantown, WV, USA

Abstract Detrital zircon (DZ) analysis has become the standard tool for source-to-sink sediment routing studies at many spatial and temporal scales. In North American source-to-sink studies, DZ distributions are commonly classified according to the presence/absence and proportions of DZ age groups associated with North American crustal provinces as well as peri-Gondwanan and Cordilleran terranes. Although such a classification scheme is descriptive, these age groups typically do not uniquely identify most recent DZ source areas. Using a compilation of >19,000 individual DZ ages for Mesoproterozoic-Paleogene strata of the northern Rocky Mountains, including 2,053 new analyses from the Paleogene Renova Formation and its equivalents in southwestern Montana, we demonstrate periodic derivation of first-cycle DZ from crystalline sources and widespread recycling of poly-cycle DZ from sedimentary sources over multimillion-year timescales. Results show that (1) DZ age distributions become increasingly complex between Mesoproterozoic and Paleogene time with the introduction of new DZ sources to the study area, but (2) once an age group appears in the northern Rocky Mountains stratigraphy, grains of that age persist up-section. These trends show that most DZ age groups are spatiotemporally ubiquitous and nonunique. We largely attribute this to periodic, tectonically induced recycling of DZ into progressively younger sedimentary systems, rather than prolonged derivation of DZ from crystalline basement sources, a trend that reflects the growth of increasingly complex topography associated with the North American Cordillera.

1. Introduction

The durability and widespread occurrence of detrital zircon (DZ) in orogenic belts and sedimentary systems make DZ analysis attractive for studies of paleohydrography and associated tectonic/climatic controls (Cawood et al., 2012; Romans et al., 2016), with the database of existing DZ data increasing exponentially since the mid-1990s (Sharman et al., 2018; their figure 1). Although sediment provenance data have been an integral component of paleogeographic and sediment routing studies for decades (Dickinson et al., 1983), the endurance of DZ grains has greatly augmented our ability to assess complex sedimentation patterns and histories, especially those that include sediment recycling and/or long transport distances. A recent example is the use of large DZ data sets from North American continental margins to interpret the Cretaceous to modern paleohydrography of the continent (Blum & Pecha, 2014; Fildani et al., 2018; Sharman et al., 2016; among others).

The spatially integrated provenance records of continental margin successions are extremely valuable for assessing the effects of broad external controls (orogenesis and climatic change) on sediment routing and deposition. However, they may also subdue hydrographic complexities associated with headward parts of drainage basins owing to the downstream evolution of provenance signals (Ingersoll et al., 1993; Romans et al., 2016). Interpretations of hinterland drainage configurations, transport pathways, and paleolandscapes from continental margin data sets are inherently limited by existing knowledge and/or assumptions regarding distant sediment source areas, the lithologies and detrital compositions of those sources, and provenance signal dilution along the source-to-sink pathway.

The North American Cordillera and Western Interior region host a complex assemblage of Archean to Cenozoic lithologies that supply both first-cycle DZ (from crystalline sources) and poly-cycle DZ (from clastic sedimentary sources) to hinterland watersheds. While individual igneous sources produce relatively simple DZ age distributions that reflect crystallization age, recycling of sedimentary sources typically generates polymodal age distributions with components that match a combination of multiple sources (e.g., Gehrels et al., 2011; Link et al., 2005). This highlights a critical concept that directly affects DZ provenance interpretations but is commonly minimalized in paleodrainage studies: A given DZ age typically reveals the age of its original crystalline source, even if it is most recently recycled from a younger sedimentary source. This potential disconnect between DZ age and most recent DZ source significantly complicates the interpretation of DZ data, especially if additional provenance or paleogeographic information is lacking.

We present a compilation of DZ data (19,771 individual analyses) for the Mesoproterozoic-Paleogene stratigraphy of the southwestern Montana sector of the North American Cordillera (Figures 1 and 2a). These data demonstrate a protracted history of orogenic recycling of zircon that highlights problematic aspects of current conventions and statistical methods used to compare DZ provenance data. We discuss the compiled data in reference to local Paleogene basins (recorded by the Paleogene Renova Formation and its equivalents; age follows Fields et al., 1985) that would have comprised the headwaters of at least one early Cenozoic watershed that drained high Cordilleran topography at this time. Although the study region currently hosts the headwaters of the Missouri River, a tributary to the Mississippi River and Gulf of Mexico, the Paleogene direction of outflow from the study region to terminal sinks remains ambiguous (e.g., Blum & Pecha, 2014; Sears, 2013; Sharman et al., 2016). Even so, the Paleogene topography and hydrography of the study area are interpreted to have closely paralleled the modern (Schwartz & Schwartz, 2013). This geologic framework provides a strong foundation to assess the influences of source rock type and distribution on regional provenance signatures, ultimately allowing us to demonstrate that much of the Paleogene DZ signal reflects recycling of North American basement-aged zircon grains rather than direct derivation from exposed basement sources.

2. Study Area and Geologic Background

The southwestern Montana sector of the North American Cordillera hosts lithologic assemblages (Figure 2b) that record (1) Archean-Paleoproterozoic cratonal accretion (Whitmeyer & Karlstrom, 2007); (2) Mesoproterozoic continental rifting (Link et al., 2007); (3) Cambrian-Permian passive margin development (Bond et al., 1985; Yonkee et al., 2014); (4) Triassic to early Paleocene contraction and foreland basin evolution (DeCelles, 2004; Yonkee & Weil, 2015); (5) Paleogene erosion and extensional reactivation of the Cordillera (Coney & Harms, 1984; Constenius, 1996; Schwartz et al., 2019); and (6) Neogene Basin and Range and Yellowstone-associated extension (Reynolds, 1979; Sears & Ryan, 2003). These assemblages are currently exposed in the extant Cordilleran hinterland, fold-thrust belt, and proximal foreland region.

This sector of the Cordillera is unique in that much of the modern landscape is inherited from the latest Cretaceous to the Paleogene, with the current distribution of mountainous areas and valleys closely paralleling Paleogene topography (Carrapa et al., 2019; Schwartz & Schwartz, 2013). Paleocurrent and modal sediment provenance data from Paleogene deposits of southwestern Montana and adjacent regions (the Renova Formation and equivalents, ~48–19 Ma) further reveal that Paleogene highlands were composed of rock types similar to those exposed today. Clastic sediments were locally sourced from high-topography areas to adjacent paleovalleys, which formed a fluvially integrated basin network that flowed beyond the study area (Figure 2a). Despite some structural overprint of Paleogene landscape features by Neogene extension, much of the modern landscape preserves the configuration of sediment source areas that fed material into Paleogene paleodrainages (Schwartz & Schwartz, 2013).

3. Methods: DZ Geochronology

3.1. Sampling and Analysis

We present a compilation of 19 new Paleogene and 207 published DZ samples (19,771 grains total), as well as 886 published single-mineral ages of igneous units from within the study area (Figure 3). Location information and references for new and published data are provided in supporting information Text S1. New sandstone samples from the Paleogene Renova Formation and equivalents were collected from a combination of basin margin (alluvial fan) and basin interior (axial fluvial) depositional environments to account for lateral variability in sandstone provenance. Samples were analyzed at the University of Arizona LaserChron Center by LA-ICP-MS (Text S1). Data were visualized using the Python-based toolset, detritalPy (Sharman et al., 2018).

10.1029/2019TC005810

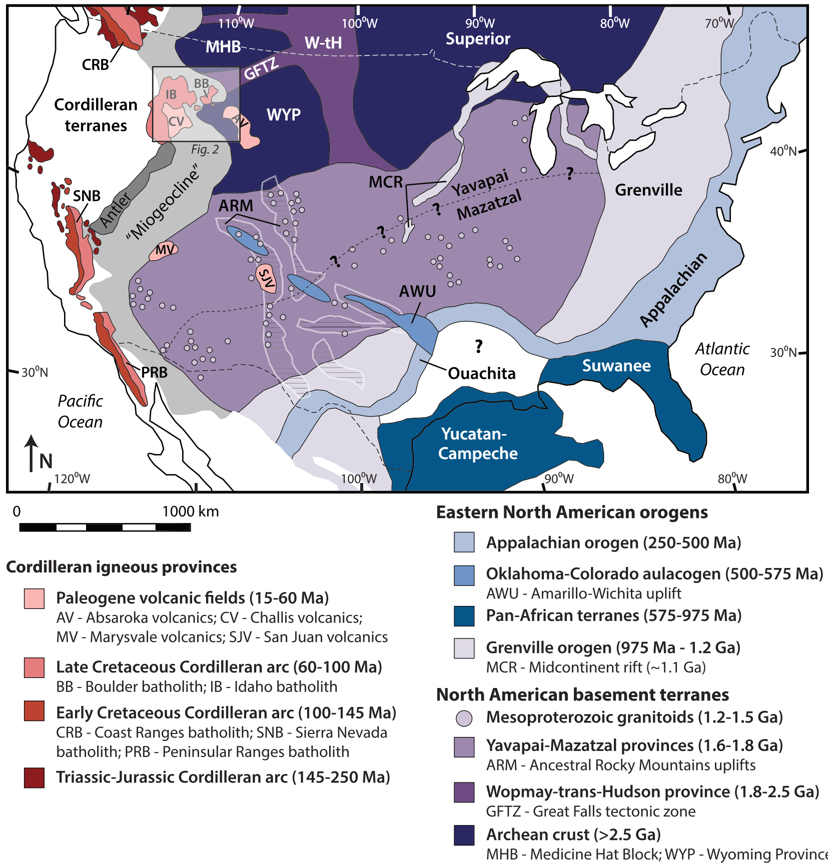

Figure 1. Map showing the study area in the context of North American basement and Cordilleran igneous provinces (modified from Chapman & Laskowski, 2019).

3.2. Interpretive Approach

Conglomerate and sandstone provenance data reveal strong spatial variation in the compositions of Paleogene deposits across the study area (Schwartz & Schwartz, 2013). This variation is due to spatial heterogeneity in (1) bedrock lithology (i.e., sediment sources), the Paleogene distribution of which was related to Sevier-Laramide structures that were subsequently modified by Paleogene erosion, volcanism, and extension; and (2) Paleogene depositional environments, which had either discrete point sources (e.g., alluvial fans) or mixed sources (e.g., axial rivers; Schwartz & Schwartz, 2013). We group all Paleogene DZ samples to generate a composite DZ distribution, or "fingerprint" ("barcode" of Link et al., 2005), of the Paleogene basin system, thereby synthetically mixing individual DZ data sets from across the study area. This approach inherently mutes local DZ signatures to provide a representative DZ signature for the entire Paleogene basin system of southwestern Montana, allowing for broader-scale comparisons between the Paleogene basin fill and proposed source assemblages.

3.2.1. Sources of First-Cycle Zircon

The study region hosts several crystalline sources of first-cycle zircon: (1) Archean to Paleoproterozoic North American basement rocks, (2) Upper Cretaceous Cordilleran arc rocks, and (3) Paleogene igneous rocks. Local North American basement terranes include the Archean Wyoming province (>2.5 Ga) and Paleoproterozoic Great Falls tectonic zone (2.5–1.8 Ga) (Figure 1; Whitmeyer & Karlstrom, 2007; Mueller et al., 2016). Upper Cretaceous Cordilleran arc rocks include the Idaho, Boulder, Pioneer, and Tobacco Root batholiths and their extrusive equivalents (e.g., Elkhorn Mountains Volcanics) (Figure 1), which were dominantly emplaced/erupted from ~90–68 Ma (Figure 3a). The batholiths were exhumed shortly following their emplacement owing to rapid uplift and erosion between ca. 65 and 53 Ma (Houston & Dilles, 2013; Schwartz & Schwartz, 2013). Paleogene post-Laramide volcanism (e.g., represented by the Challis, Dillon,

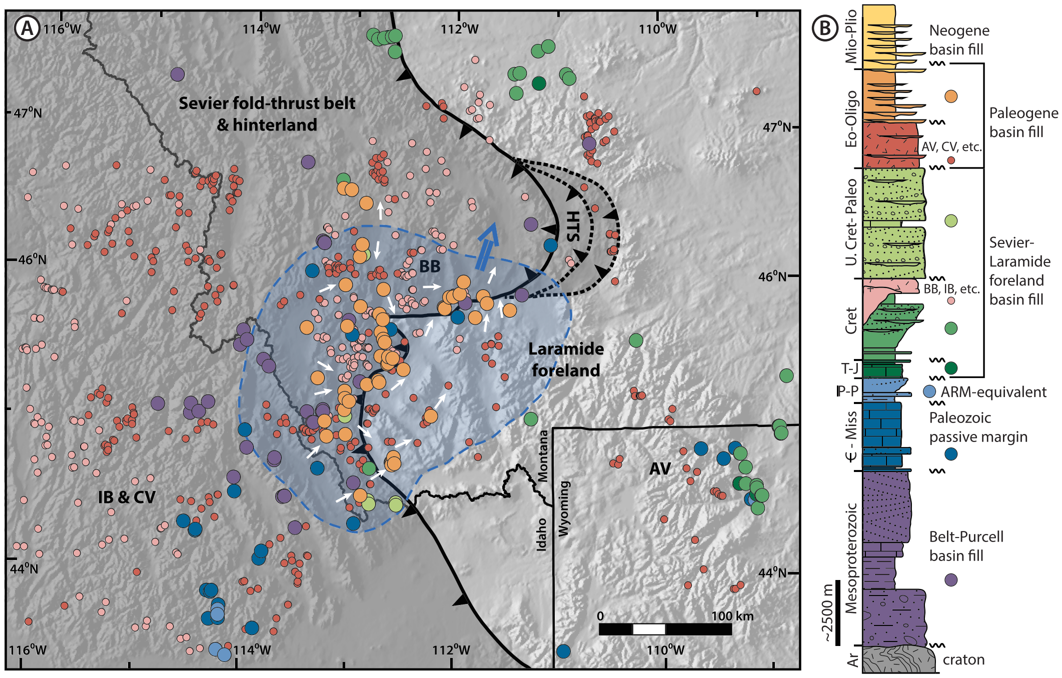

Figure 2. (a) Hillshade map of the southwestern Montana study region (including east-central Idaho and northwest Wyoming) showing the structural boundary between the Cretaceous-Paleogene Sevier fold-thrust belt and Laramide foreland province (AV = Absaroka volcanic field; BB = Boulder batholith; CV = Challis volcanic field; HTS = Helena thrust salient; IB = Idaho batholith). Large and small circles, respectively, show the distributions of detrital zircon and igneous samples discussed in the text; symbols are color coded according to the ages of host lithologies, shown in (b). The blue shaded region denotes a possible watershed boundary for the series of interconnected Paleogene basins that drained the area, with white arrows summarizing paleocurrent directions in individual basins and the blue arrow indicating a likely direction of outflow from the region (after Janecke et al., 1999; Schwartz & Schwartz, 2013; Schwartz & Graham, 2017). Please note that the extent of the watershed may be larger and more complex than depicted and that paleodrainage pathways beyond the study region are currently unknown. (b) Simplified stratigraphic column for southwestern Montana (modified from Vuke et al., 2009) that shows the relative thicknesses and lithologic characters of Mesoproterozoic-Neogene units (ARM = Ancestral Rocky Mountains).

Lowland Creek, and Absaroka volcanic fields) occurred from ~55–40 Ma (Figure 3a), coeval with exhumation of the Bitterroot and Anaconda metamorphic core complexes. Paleogene volcanism was transitional with late-stage emplacement of the Idaho batholith (Gaschnig et al., 2010) and continued locally until ~15 Ma (Figure 3a) (Fritz et al., 2007).

3.2.2. Sources of Poly-Cycle Zircon

Similar to Paleogene samples, we group samples from sedimentary sources of poly-cycle zircon to obtain their respective DZ fingerprints (individual data sets are shown in Text S2). Potential sources include the following tectonostratigraphic units (Figure 2b): (1) the Mesoproterozoic Belt Supergroup, (2) Paleozoic (Cambrian to Mississippian) "miogeoclinal" strata, (3) Pennsylvanian-Permian strata deposited coeval with uplift of the Ancestral Rocky Mountains, (4) Triassic-Jurassic strata of the incipient Sevier foreland basin, (5) Cretaceous strata of the Sevier foreland basin, and (6) Upper Cretaceous to lower Paleocene synorogenic strata deposited proximal to the Sevier thrust front and Laramide intraforeland uplifts of southwestern Montana. We separate Cretaceous-Paleocene synorogenic units (the conglomeratic Beaverhead Group) from more distal Cretaceous foreland strata because of their exclusively local sources in the adjacent fold-thrust belt or Laramide uplifts (Haley & Perry, 1991), compared to foredeep strata that received a mixture of sediment from more distant sources. Approximately one third ($N = 59/174$) of compiled DZ samples representing potential sediment sources to the Paleogene basin network are from within established watershed boundaries of the Paleogene basin system (Figure 2a). DZ samples of potential sediment sources were also compiled from adjacent areas in Idaho, northern Montana, and Wyoming as potential proxies for age-equivalent units within the watershed (Figure 2a). Importantly, we note that some tectonostratigraphic

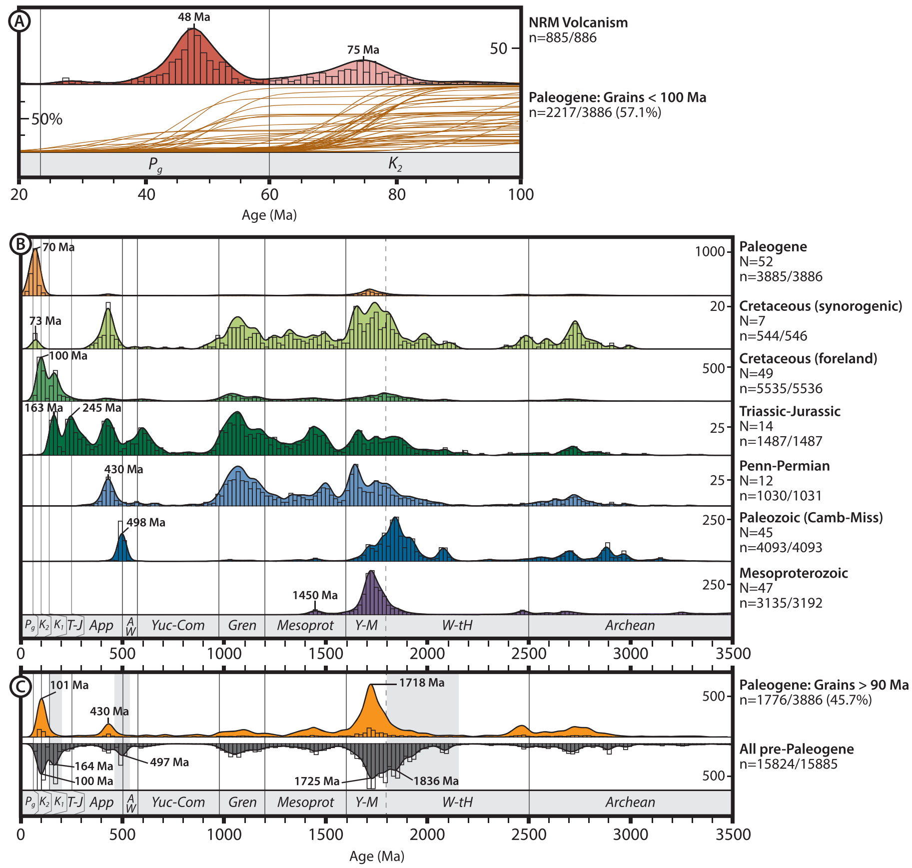

Figure 3. Detrital mineral distributions. (a) Kernel density estimate (KDE; bandwidth = 2; histogram bins = 1 Ma) of compiled Late Cretaceous-Paleogene single-mineral ages of igneous units within/near the study area, demonstrating an ~75 Ma peak related to emplacement of Cordilleran batholiths (i.e., the Idaho, Boulder, Pioneer, Tobacco Root batholiths, and their satellites) and an ~48 Ma peak related to eruption of post-Laramide volcanic fields (i.e., Challis, Absaroka, Lowland Creek, and Dillon). The lower panel shows excerpts of cumulative curves for 52 Paleogene detrital zircon samples from the study region. Note that all Paleogene detrital zircon samples contain at least 10% northern Rocky Mountains (NRM) igneous ages and that these ages account for more than 50% of all grains analyzed in Paleogene samples. (b) Composite nonnormalized KDEs (bandwidth = 20; histogram bins = 20 Ma) for the seven tectonostratigraphic units discussed in this study; the plots are color coded according to the tectonostratigraphy shown in Figure 2b. (c) Comparison of normalized KDEs for the modified Paleogene spectrum (all grains >90 Ma) and a composite of all pre-Paleogene samples (bandwidth = 20; histogram bins = 20 Ma). Light gray areas highlight apparent disparities between the two spectra. All plots are subdivided according to the ages of North American basement and Cordilleran terranes; see text for details.

units contain relatively small volumes of sandstone because the cumulative thickness of the unit is small (e.g., Pennsylvanian-Permian and Triassic-Jurassic units) and/or the unit is dominated by limestone or mudrocks (e.g., Cambrian-Mississippian and Triassic-Jurassic units; Figure 2b). Sediment contributed from carbonates and mudrocks is likely underrepresented in the DZ distributions of Paleogene samples, but these lithologies have been observed as clasts in outcrop and thus were substantive sources of sediment to the Paleogene basin network (Schwartz & Schwartz, 2013).

3.2.3. DZ Age Domains

To facilitate comparisons of age spectra, we subdivide the composite DZ distributions according to established first-cycle DZ age ranges of North American crustal provinces and the Cordilleran arc (Figures 1 and 3; after Whitmeyer & Karlstrom, 2007; Gehrels et al., 2011; Sharman et al., 2014; Chapman & Laskowski, 2019; this study): Archean crustal provinces (>2.5 Ga); the Paleoproterozoic Wopmay-Trans-Hudson (2.5–1.8 Ga) and Yavapai-Mazatzal (1.8–1.6 Ga) provinces; Mesoproterozoic magmatic provinces (1.6–1.2 Ga, of which 1.6–1.5 Ga ages correspond to the North American magmatic gap and were likely derived from the Siberian, Australian, and/or Antarctic cratons; Ross & Villeneuve, 2003; Link et al., 2007;

Stewart et al., 2010); the Grenville orogen (1.2 Ga to 975 Ma); the Yucatan-Compeche terrane (975–575 Ma); the Amarillo-Wichita uplift (575–500 Ma); the Appalachian orogen (500–250 Ma, of which 500–490 Ma ages correspond to Cambrian plutons located in central Idaho; Link et al., 2017); the Triassic-Jurassic (250–145 Ma) and Lower Cretaceous Sierra Nevada arc (145–100 Ma; herein K_1); the Upper Cretaceous northern Rocky Mountain arc (100–60 Ma; herein K_2); and Paleogene volcanics (60–15 Ma).

4. Results

4.1. Paleogene Samples

Individual DZ distributions for the Paleogene Renova Formation and equivalents show great spatial variability (Figure 3a) that mimics the heterogeneity of sandstone/conglomerate modal compositions (Schwartz & Schwartz, 2013). This variability is attributed to spatial heterogeneity in sediment sources and degrees of sediment mixing within various depositional environments of the Paleogene watershed (Figure 2a). Notably, all samples contain ≥10% Paleogene (60–15 Ma) to Late Cretaceous (100–60 Ma) grains (Figure 3a), reflecting high-volume input of first-cycle DZ from Paleogene volcanic fields and exhumed Upper Cretaceous arc rocks. Accordingly, the composite Paleogene distribution is dominated by northern Rocky Mountains igneous ages (54% of DZ are 100–15 Ma; $n = 2{,}110/3{,}886$) with subsidiary Appalachian, Yavapai-Mazatzal, and Archean components (Figure 3b).

4.2. Mesoproterozoic-Paleogene Composite Spectra

Figure 3b shows composite DZ distributions for the Mesoproterozoic-Paleogene tectonostratigraphic units. We characterize the succession with three notable observations.

(1) Age distributions become increasingly polymodal through time (Figure 3b). The Mesoproterozoic and lower Paleozoic spectra include relatively few age modes, mainly Archean, Paleoproterozoic and Mesoproterozoic, and ~500 Ma peaks. The Pennsylvanian-Permian spectrum records a conspicuous increase in modality with the addition of Appalachian, Grenville, and other Mesoproterozoic peaks. The overlying Triassic-Jurassic spectrum records increased modality with the addition of coeval Cordilleran arc ages. The Cretaceous foreland basin spectrum is similarly dominated by coeval arc ages but retains smaller proportions of all older age groups, which are better revealed by the Cretaceous-Paleocene synorogenic spectrum because it lacks a dominant arc component. The Paleogene spectrum is similar to the Cretaceous foreland basin spectrum in that it is dominated by relatively young, Late Cretaceous-Paleogene igneous ages, also retaining smaller proportions of all older age groups.

(2) When present, Cordilleran arc-derived zircon tends to significantly outnumber older ages (Figure 3b). The Triassic-Jurassic, Cretaceous foreland, and Paleogene spectra demonstrate strong arc peaks (respectively at ~245 and 163, 100, and 70 Ma; Figure 3b) that broadly correspond to their depositional ages. These age groups respectively account for approximately 11%, 44%, and 57% of all grains in those units. The large proportions of syndepositional DZ significantly obscure the presence of older age groups, particularly in the Cretaceous foreland and Paleogene spectra.

(3) Once an age group appears in the tectonostratigraphic sequence, grains of that age persist up-section (Figure 3b). For example, the Mesoproterozoic spectrum is dominated by Yavapai-Mazatzal ages (1.8–1.6 Ga). Those ages are present in a lower proportion in the Paleozoic spectrum and then remain an obvious component in all overlying spectra. Similarly, once Grenville ages appear in the Pennsylvanian-Permian spectrum, there is an obvious presence in overlying spectra. The Triassic-Jurassic arc peak dominates the Triassic-Jurassic spectrum, is strong (but diminished) in the Cretaceous spectrum, and is minor in the Paleogene spectrum. It is worth noting that individual samples may not adhere to this trend, which we attribute to lateral variability in the DZ distributions of individual tectonostratigraphic units.

5. Discussion

5.1. Comparison of Paleogene to Pre-Paleogene Spectra

Modal clast compositions indicate that the pre-Paleogene tectonostratigraphic units shown in Figure 2b were sources of coarse-grained sediment (i.e., sand and coarser) to the Paleogene basin network (Schwartz & Schwartz, 2013). Accordingly, the composite Paleogene DZ spectrum should mimic a composite of all older tectonostratigraphic units, but the high proportion (54%) of northern Rocky Mountains igneous ages (~100–

15 Ma) mutes the presence of older age modes (Figure 3b). Since northern Rocky Mountains igneous ages corresponding to the Idaho-Boulder batholith complex and Paleogene volcanic fields are absent in all older spectra and are interpreted to have been locally derived, we modify the Paleogene spectrum to omit all ages <90 Ma. Figure 3c mirrors the modified Paleogene spectrum and a composite of all Mesoproterozoic-Upper Cretaceous samples. The modified Paleogene spectrum strongly resembles the pre-Paleogene composite: Yavapai-Mazatzal ages are dominant, followed by Cretaceous ages, with lower proportions of Appalachian, Grenville, Mesoproterozoic, and Archean ages (Figure 3c). Notably, the modified Paleogene spectrum lacks the robust Triassic-Jurassic (~164 Ma), Late Cambrian (~500 Ma), and Paleoproterozoic (~2.2–1.8 Ga) modes that are obvious in the composite pre-Paleogene spectrum (Figure 3c). These ages are present, but respectively comprise only 0.4% (17 grains between 250 and 145 Ma), 0.6% (25 grains between 550 and 450 Ma), and 4.0% (156 grains from 2.2–1.8 Ga) of all ages (3,886 grains). We attribute their relative paucity to three factors.

(1) There is lateral variability in some of the DZ distributions of pre-Paleogene sedimentary units that sourced the Paleogene basins. For this reason, some of the compiled DZ samples of source units may not be representative of their equivalents within the study area that were actual point sources to the Paleogene basin system. For example, Jurassic-Lower Cretaceous foreland basin deposits in northern Montana (Fuentes et al., 2009, 2011; Leier & Gehrels, 2011; Quinn et al., 2018) and Wyoming (May et al., 2013) commonly contain a ~165 Ma peak, but Lower Cretaceous units that have been sampled within the study area lack a ~165 Ma peak (Laskowski et al., 2013; Link et al., 2008). Similarly, Cambrian sandstones from southeastern Idaho contain a strong ~500 Ma peak (Link et al., 2017), but ~500 Ma grains remain undocumented in more local Cambrian sandstones (Link et al., 2016, 2017; Sears et al., 2010). These results demonstrate how the compositional variability in sources of poly-cycle DZ may affect DZ signatures in a receiving basin, as well as allude to the hindrance on sediment mixing by a complex Paleogene landscape.

(2) Some samples compiled from the literature as proxies for local pre-Paleogene units were likely collected from areas beyond the watershed that occupied the Paleogene basin network, that is, beyond the paleodrainage basin marked in Figure 2a. Previous provenance, paleodispersal, and paleotopographic data demonstrate that southwest Montana was characterized by a rugged Paleogene topography comprising a network of relatively narrow, fluvially interconnected basins bounded by high-relief (≥2 km) mountainous areas (Schwartz et al., 2019; Schwartz & Schwartz, 2013). Each topographically high area was a point source of sediment to adjacent basins, and sediment from those sources was mixed as it was transported downstream. As such, the presence of a rugged Paleogene topography limited the clastic input of some potential source rocks. For example, the westernmost boundary of the Paleogene watershed remains unclear. Existing sediment provenance data indicate that the western boundary varied through time; hinterland rivers drained the eastern Challis volcanic field into southwestern Montana until ~45 Ma, after which the drainage network was beheaded by extension (Janecke et al., 1999; Schwartz et al., 2019). Ordovician, Devonian, and Mississippian sandstones from Idaho, west of the known watershed boundary (Figure 2a), contain strong ~500 Ma and ~2.2–1.8 Ga age modes (Baar, 2009; Beranek et al., 2016) that are minor in Paleogene samples. Thus, the relative paucity of these ages in the Paleogene spectrum may support periods of topographic/hydrographic isolation from specific sediment source areas.

(3) Finally, some tectonostratigraphic units are thin and/or contain only limited intervals of coarse-grained siliciclastic sediment (Figure 2b) and were therefore unlikely to contribute large volumes of DZ to the Paleogene basin system. For example, local Jurassic-Lower Cretaceous foreland basin units are thin, mudstone dominated and have limited exposure within the Paleogene watershed (Vuke et al., 2009). In addition, Devonian-Permian units in the study area are dominantly limestone (Vuke et al., 2009), unlike their sandier equivalents to the east and west (e.g., Beranek et al., 2016). It is reasonable that such units are underrepresented in the Paleogene DZ spectrum due to their inherently low zircon fertility and/or dilution by higher-volume sources of DZ.

5.2. Orogenic Recycling of DZs

5.2.1. First- Versus Poly-Cycle Contributions: Insights From MDS

The sustained presence of DZ age groups in the Cordilleran stratigraphy (Figure 3b) prompts consideration of first-cycle derivation versus recycling of DZ grains. The presence of any DZ age group may reflect erosion of crystalline sources (first-cycle DZ), erosion of older sedimentary rocks containing DZ of that age (poly-

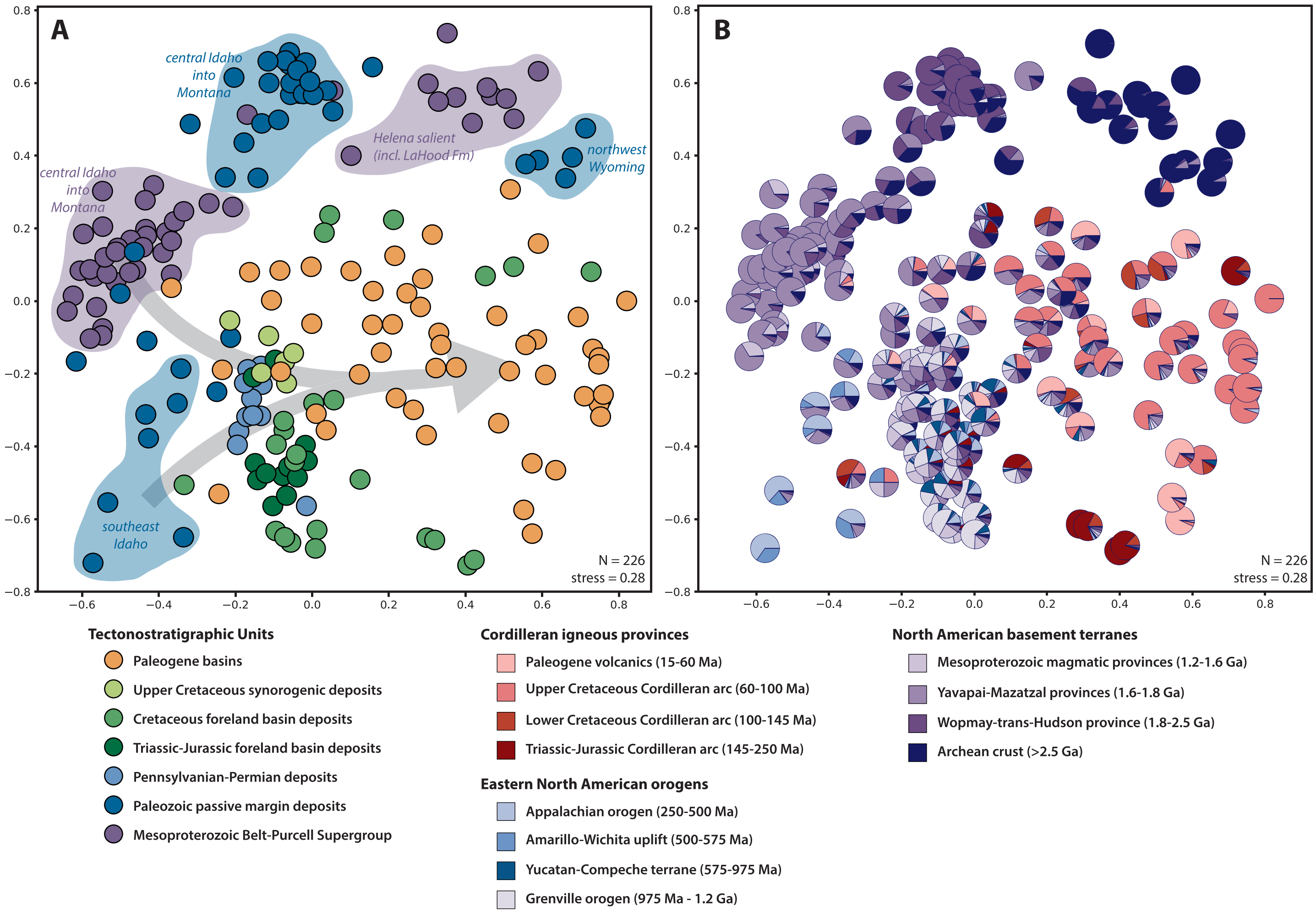

Figure 4. Multidimensional scaling analysis of all Mesoproterozoic-Paleogene samples discussed in this study, color coded according to tectonostratigraphic unit (a) and showing individual DZ distributions as pie diagrams (b). Panel (a) shows that although there is lateral variability in sample composition within each tectonostratigraphic unit, there is retention of compositional characteristics through time (symbolized by gray arrow). Panel (b) highlights the evolution from basement-dominated to arc-dominated DZ distributions within the study area, as well as shows the persistence of different DZ ages through time.

cycle DZ), or a combination of both. Generally, crystalline sources of first-cycle DZ may become available to adjacent basins during active volcanism, unroofing of extant igneous provinces, and/or tectonic or erosional exhumation of basement terranes. Sedimentary sources of poly-cycle DZ may appear as a result of tectonic uplift in orogenic belts or erosion of overburden. Large-scale drainage reorganization may also introduce both types of DZ from distant sources to a basin system.

The time-transgressive similarities in Cordilleran DZ spectra (Figure 3b) largely reflect the recycling of DZ via tectonic reorganization of predecessor basin systems, rather than input of first-cycle DZ by crystalline sources. Progressive inheritance of poly-cycle DZ is visually highlighted by nonmetric multidimensional scaling (MDS; Figure 4) analysis of all compiled DZ samples. Nonmetric MDS facilitates a quantitative comparison of intersample dissimilarity measures in which the exact coordinate values of each sample point in MDS space carry no specific meaning, but the distance between any two samples (i.e., points in Figure 4) in unitless space reflects their relative similarity/dissimilarity (Vermeesch, 2013; see Supporting Information S1 for additional details). Figure 4 presents MDS plots of all 226 DZ samples utilized in this study. The two plots show the same MDS-space distributions of age data, in the first case color-coded according to tectonostratigraphic unit (Figure 4a) and in the second case showing pie charts of individual DZ sample compositions (Figure 4b).

The MDS distributions of sample sets shown in Figure 4 illustrate a marked evolution in provenance from Mesoproterozoic-Paleogene time but also highlight temporally persistent similarities. There is distinct lateral variability in the DZ distributions of Mesoproterozoic and Paleozoic samples, shown by a broad, arcuate distribution of samples in the northern and western quadrants of the MDS space (Figure 4a). Mesoproterozoic and Paleozoic samples are variably clustered according to differences in proportions of Archean, Paleoproterozoic, and Mesoproterozoic DZ constituents (Figure 4b), largely corresponding to spatially distinct outcrop areas in Idaho, Montana, and Wyoming (Figure 4a). Each successive sample set is progressively offset to the right from the Mesoproterozoic and Paleozoic samples that are located in the southwest quadrant of the MDS space: The Pennsylvanian-Permian, Triassic-Jurassic, and Cretaceous sample sets show incremental offset to the right, whereas the majority of Paleogene samples show more obvious offset (Figure 4a). In addition, there is a temporal trend in clustering/dispersion within sample sets, in which Pennsylvanian-Permian and Triassic-Jurassic samples are tightly clustered, Cretaceous samples are clustered into two apparent groups, and Paleogene samples are evenly dispersed throughout the central part of the MDS space (Figure 4a).

These trends highlight three important facets of the data set. (1) Each new tectonostratigraphic unit retains DZ components of predecessor units but also includes new DZ age groups. For example, Mesoproterozoic and Paleozoic samples are dominated by Mesoproterozoic and older grains (Figure 4b). Pennsylvanian-Permian, Triassic-Jurassic, Cretaceous, and Paleogene samples share those DZ age groups but also record the progressive introduction of eastern Laurentian (Grenville and Appalachian) followed by Cordilleran arc ages to the study area (Figure 4b). (2) The apparent emanation of sample points from the western hemisphere of the MDS space suggests an enduring affinity of younger sample sets to Mesoproterozoic-Paleozoic units exposed in central-southeast Idaho and southwestern Montana (Figure 4a). It is not until Late Cretaceous-Paleogene time that DZ samples cluster closer to Mesoproterozoic-Paleozoic samples from the Helena salient and northwestern Wyoming (Figure 4a), which is likely linked to long-term paleodrainage evolution within the study area. (3) Finally, the increasing dispersion of sample groups in the MDS space reflects both the temporal evolution of available sediment sources and the development of a progressively complex Cordilleran landscape beginning in the Cretaceous.

5.2.2. Implications for the Growth of Cordilleran Topography

The temporal trends shown in Figures 3b and 4 suggest strong similarities in the DZ fingerprints of successive tectonostratigraphic units within the study area. Adding independent geologic context for each time interval documents the prevalence of DZ recycling for much of the past 1.5 Ga in western North America. Fundamentally, the presence of a DZ age group in a given tectonostratigraphic unit requires availability of an associated DZ source and a sedimentary connection to that source. Figure 5 schematizes the availability of sources of first- and poly-cycle DZ to the study area through time based on a combination of DZ, sandstone petrography, paleoenvironmental, and structural interpretations.

Mesoproterozoic strata are largely characterized by presumably first-cycle Archean to Mesoproterozoic DZ derived from exposures of North American cratonic basement, Belt Supergroup volcanic rocks, and non-North American sources in Siberia, Australia, and/or Antarctica (Figure 5a; Ross & Villeneuve, 2003; Link et al., 2007; Stewart et al., 2010; Mueller et al., 2016). Syndepositional basement exposure within/near the study area is corroborated by the presence of abundant basement-derived metamorphic and meta-igneous cobbles and boulders in the feldspathic LaHood Formation (McMannis, 1963), at the base of the Belt Supergroup in the Helena thrust salient. The LaHood Formation also contains abundant Archean DZ (Figure 4a) sourced from the Wyoming province. Following widespread Neoproterozoic cratonal denudation and the formation of the Great Unconformity, lowest Paleozoic marine sandstones were sourced from beveled North American basement terranes, as well as locally from underlying Mesoproterozoic sedimentary units, which, respectively, provided first- and poly-cycle Cambrian and Mesoproterozoic-Archean zircon to the lower Paleozoic section (Figure 5b; Baar, 2009; May et al., 2013; Link et al., 2016, 2017; Malone et al., 2017). Modal provenance data support this interpretation, showing increased feldspar concentrations where the Cambrian Flathead Sandstone unconformably overlies quartzofeldspathic basement and Mesoproterozoic strata (Graham & Suttner, 1974; McLane, 1971, 1972; McMannis, 1963). However, Late Cambrian to Ordovician marine transgressions blanketed much of the North American craton with a veneer of shallow marine sediments (Peters & Gaines, 2012; Sloss, 1963), essentially eliminating North American cratonic rocks as widespread sources of first-cycle DZ. In the study area, this is reflected petrographically

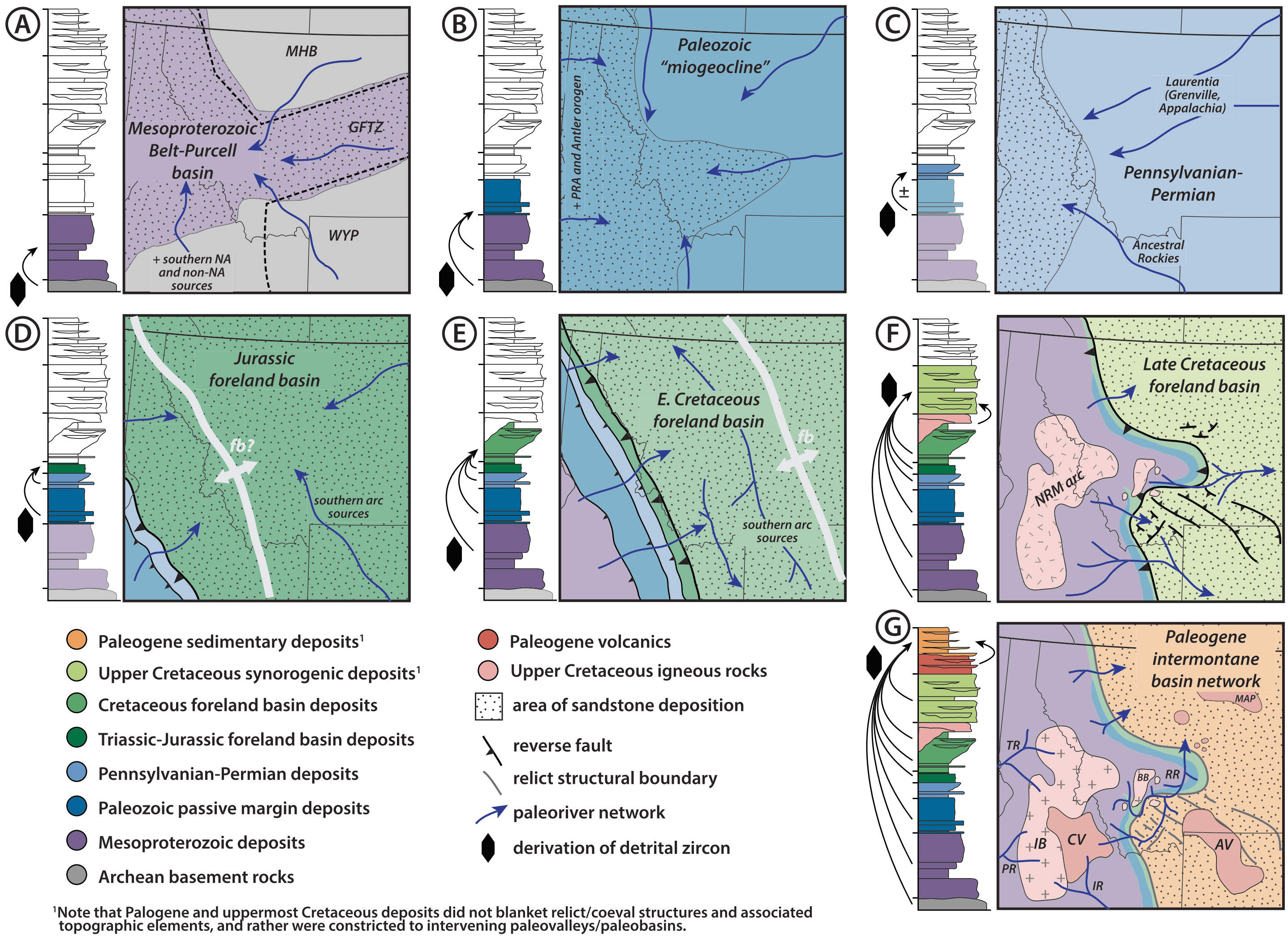

Figure 5. Generalized paleogeographic maps of the study area for (a) Mesoproterozoic, (b) Paleozoic, (c) Pennsylvanian-Permian, (d) Triassic-Jurassic, (e) Early Cretaceous, (f) Late Cretaceous, and (g) Paleogene time. The series of maps schematize the extent of exposure of potential source rocks (solid colors) and areas of deposition (stippled). Pre-Paleogene paleogeographic representations are largely informed by references cited in the text. Stratigraphic columns depict the recycling of older units into progressively younger units for each time period. AV = Absaroka Volcanic Supergroup; BB = Boulder batholith; CV = Challis Volcanics; fb = forebulge (approximate location); GFTZ = Great Falls tectonic zone; IB = Idaho batholith; IR = Idaho River (Chetel et al., 2011); MAP = Montana alkalic province; MHB = Medicine Hat block; NA = North America; NRM = northern Rocky Mountains; PR = Princeton River (Dumitru et al., 2013); RR = Renova river system (Schwartz & Schwartz, 2013; this study); TR = Tyee River (Dumitru et al., 2013); WYP = Wyoming province.

by an up-section decrease in detrital feldspar content relative to quartz (McLane, 1971, 1972). Middle Ordovician to Mississippian development of the Peace River arch and Antler orogen introduced new, western sources of first- and poly-cycle DZ to depocenters now exposed in Idaho (Baar, 2009; Beranek et al., 2016), but coeval strata in the southwestern Montana study area were dominated by carbonate environments with minor siliciclastic intervals (e.g., Figure 2b).

Pennsylvanian-Permian samples (Figure 3b) record the introduction of eastern Laurentian DZ to western North America via transcontinental paleodispersal systems, with late Mesoproterozoic to Paleozoic DZ age groups transported across the overfilled Alleghany foreland from the uplifted Grenville and Alleghany orogenic belts (Figure 5c; May et al., 2013; Link et al., 2014; Chapman & Laskowski, 2019). Archean and Proterozoic DZ were reworked from Paleozoic strata that were exhumed during uplift of the Ancestral Rocky Mountains (May et al., 2013), from local uplifted areas near/within southwestern Montana (Cressman & Swanson, 1964; Schwartz & DeCelles, 1988), and from undetermined western sources (Link et al., 2014), with possible first-cycle input from Ancestral Rocky Mountains basement exposures (Maughan, 1990).

10.1029/2019TC005810

Jurassic initiation and subsequent growth of the Cordilleran arc and foreland basin system again altered North American paleodispersal patterns (DeCelles, 2004), becoming a major source of sediment to basins in western North America. First- and poly-cycle DZ were derived from the Jurassic arc and incipient Cordilleran fold-thrust belt, respectively, and were carried to the southwestern Montana region by northward-directed, longitudinal paleodispersal systems within the Sevier foreland basin complex (after Fuentes et al., 2009, 2011; May et al., 2013) as well as via aerial delivery. Poly-cycle DZ may also have been reworked from local, incipient intraforeland uplifts associated with the early reactivation of Laramide intraforeland structures beginning in Jurassic time (Figure 5d; after DeCelles, 1986; Schwartz & DeCelles, 1988; Meyers & Schwartz, 1994).

Progressive growth of the Cordilleran arc and eastward propagation of the Sevier fold-thrust belt during Cretaceous time resulted in an increasingly complex topography across western Montana (Figure 5e). The presence of Sierra Nevada arc-aged DZ in Lower Cretaceous samples from northwest and central Montana (Fuentes et al., 2009, 2011; Leier & Gehrels, 2011; Quinn et al., 2018) suggests continued long-distance transport of DZ from the southern arc along the axis of the Sevier foreland basin, but a lack of those ages in Lower Cretaceous samples from southwest Montana supports local topographic isolation from the basin-axial paleodispersal system (Figure 5e). Growing topographic complexity within the Early Cretaceous Sevier foreland is supported by the nearly bimodal distribution of Cretaceous samples in Figure 4, as well as by paleodispersal and modal provenance data that illustrate partitioning of paleoriver systems within the southwestern Montana foreland associated with the early growth of Laramide intraforeland structures (DeCelles, 1986; Schwartz & DeCelles, 1988).

Upper Cretaceous foreland basin deposits record initiation of the northern Rocky Mountains arc (Figure 3a), regression of the Western Interior Seaway from western Montana (DeCelles, 2004), continued regional uplift of Laramide intraforeland structures (Carrapa et al., 2019), and subsidence of Laramide intraforeland basins, as well as a transition to localized sediment derivation from the Sevier-Laramide orogen (Figure 5f). The northern Rocky Mountains arc (today represented by the Idaho-Boulder batholith complex) and fold-thrust belt respectively sourced abundant first- and poly-cycle DZ to the foreland basin (e.g., Scarberry & Yakoklev, 2018). Continued Maastrichtian-Paleocene emergence of Laramide intraforeland structures (Carrapa et al., 2019) locally unroofed North American basement rocks as sources of first-cycle DZ, recorded by the presence of metamorphic clasts in synorogenic conglomerates (Haley & Perry, 1991; Perry et al., 1988).

Late-stage Sevier-Laramide deformation in early Paleocene time was temporally associated with fluvial erosion of the contractional landscape, concentrated along zones of structural and stratigraphic weakness in the Sevier-Laramide orogen (Schwartz & Schwartz, 2013). Although Paleogene physiography largely resembled that of the Sevier-Laramide orogen, erosion and local extension further enhanced the relief and complexity of the Paleogene post-Laramide basin network (Schwartz et al., 2019). During this time, the volcanic carapace of the northern Rocky Mountains arc was unroofed to expose Upper Cretaceous batholiths (Figure 5g; Houston & Dilles, 2013; Schwartz & Schwartz, 2013) as voluminous sources of first-cycle DZ. Similarly, Archean-Paleoproterozoic basement rocks were reexposed in intraforeland uplifts, as indicated by the presence of basement-derived metamorphic clasts within alluvial fan and fluvial deposits of the Paleogene Renova Formation (Schwartz et al., 2011; Schwartz & Schwartz, 2013; Stroup et al., 2008). Thus, throughout the Paleogene, voluminous first-cycle DZ originated from the exhumed Upper Cretaceous batholiths and basement uplifts, as well as from nearby Paleogene volcanic fields (Figure 3a), while poly-cycle DZ was synchronously derived from pre-Paleogene strata exposed in extant Sevier-Laramide structures (Figure 5g). The topographic complexity of the study region coupled with lateral heterogeneity in sediment sources resulted in spatially variable DZ signatures within the Paleogene basin network (Figure 4).

5.2.3. Implications for North American Source-to-Sink Studies

In North American DZ studies, it is common to subdivide DZ distributions according to North American crustal province ages (Figure 1) to compare the presence/absence and proportions of DZ age groups among samples. For example, many continental margin-based paleodrainage studies (e.g., Blum & Pecha, 2014; Sharman et al., 2016) use subdivision schemes similar to that shown in Figure 3. Although convenient, this approach is misleading because basement-aged grains are not uniquely derived from their associated basement provinces. For example, we document that detrital Yavapai-Mazatzal grains first appear in Mesoproterozoic strata and are common through the Paleogene (Figure 3b), but the Yavapai-Mazatzal crustal province was largely eliminated as a source of first-cycle DZ by Late Cambrian time (e.g., Sloss,

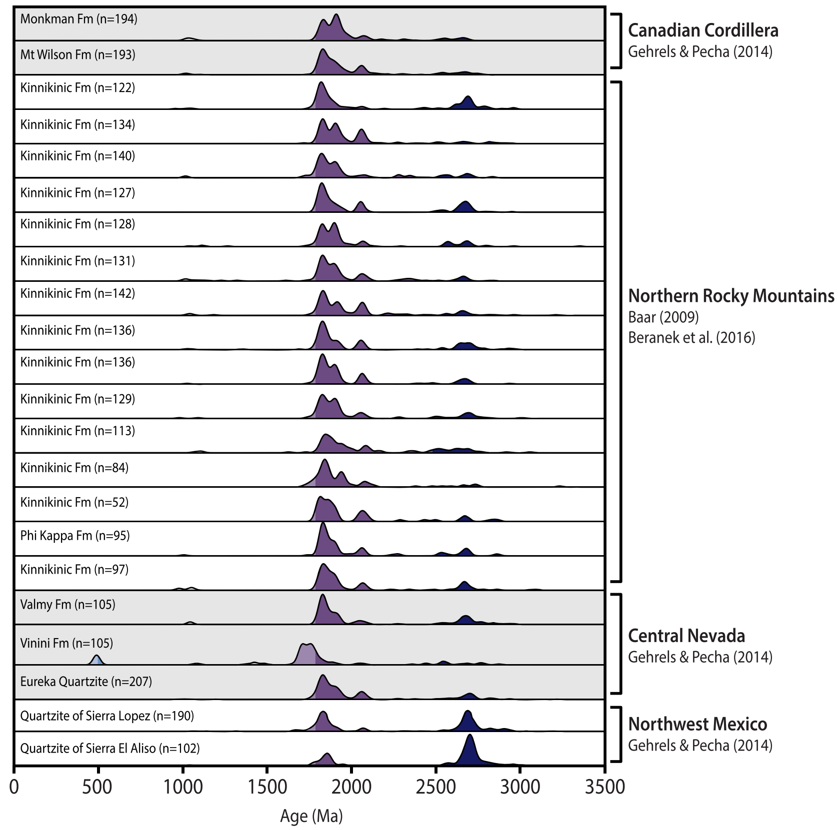

Figure 6. Normalized KDEs of detrital zircon data for Ordovician sandstones that occur in the North American Cordillera between northern Canada and northern New Mexico (distance >2,000 km). Note that with few exceptions, the presence and relative proportions of Archean and Proterozoic DZ distributions are strikingly similar. Age groups are color coded according to the keys shown in Figures 1 and 4b.

1963). Similarly, detrital Triassic-Jurassic arc grains appear in age-equivalent strata and persist through the Paleogene in smaller proportions, but paleogeographic reconstructions support Early Cretaceous hydrographic isolation of the study area from the Triassic-Jurassic arc (DeCelles, 2004; Schwartz & DeCelles, 1988). Accordingly, neither Yavapai-Mazatzal nor Triassic-Jurassic DZ in Paleogene samples can be first-cycle DZ and thus are not diagnostic of crystalline sources of sediment to the Paleogene basin network; rather, their presence requires recycling from a sedimentary source. The temporal persistence of DZ age groups may be further complicated by lateral consistency in the DZ age distributions of source units, sometimes over many hundreds to thousands of kilometers. For example, Figure 6 shows that Ordovician samples from the study area are very similar to coeval units reaching from the Canadian Cordillera to northwest Mexico, revealing a potential >2,000 km-long, sedimentary line source of Paleoproterozoic DZ.

Ultimately, detailed paleogeographic and paleohydrographic interpretations are limited by the ubiquity of pre-Cordilleran grains and the nonuniqueness of their most recent sources relative to the basin system in question. While there is value in subdividing DZ distributions according to North American basement ages for a strictly comparative measure, the spatiotemporal nonuniqueness of those ages prohibits their use as source area “fingerprints” without additional information. This limitation has major implications for how these age groups may be used for intersample comparisons and strongly reinforces (1) the significance of site-specific geologic/paleogeographic context when interpreting DZ distributions, (2) the value of additional provenance indicators (e.g., modal compositions of conglomerate or sandstone), (3) the need to compare DZ distributions to those of older strata that may have sourced a given basin, (4) the importance of identifying relatively rare or unique age groups (or combinations thereof) via large-*n* data sets (e.g., Pullen et al., 2014) that may reveal specific source areas, (5) the need for statistically rigorous methods for characterizing and comparing DZ distributions (e.g., Saylor et al., 2019; Sharman & Johnstone, 2017; Sundell & Saylor, 2017; Vermeesch & Garzanti, 2015), and (6) the utility of multiproxy approaches to deconvolve complex provenance data (e.g., Gehrels & Pecha, 2014).

6. Conclusions

Mesoproterozoic to Paleogene strata exposed in the southwestern Montana sector of the North American Cordillera can be subdivided into six tectonostratigraphic successions that record the tectonic evolution of western North America. Our DZ data compilation for the six successions (including 19,771 individual analyses) illustrates the following:

1. Composite DZ spectra for the Mesoproterozoic-Paleogene successions reflect a combination of periodic, first-cycle DZ derivation from crystalline sources and multistage recycling of poly-cycle DZ from older sedimentary units.
2. DZ age distributions become increasingly complex through time, but once an age group appears in the Mesoproterozoic-Paleogene tectonostratigraphic sequence, most grains of that age persist up-section (Figure 3b). Thus, North American basement ages are ubiquitous in Cordilleran strata, and their presence in a given sample is insufficient to identify unique source areas in many cases.
3. MDS analysis of all 226 samples used in this study quantitatively demonstrates an "inheritance" of DZ age distributions through time, in which successive sedimentary units share DZ characteristics with predecessor units (Figure 4). These compositional trends combined with additional geological context allow for informed interpretations regarding DZ input by first- versus poly-cycle sources, as well as broad-scale determinations of sediment routing in the northern Rocky Mountains (Figure 5).

The synthesis of DZ data from Paleogene deposits of the northern Rocky Mountains presented herein affords a hinterland comparison to studies of coeval deposits from continental margins. It both highlights the spatial variability in DZ distributions that is possible for hinterland areas, as well as illustrates how such variability may be muted during sediment "mixing" along the source-to-sink pathway (Figures 3a and 3b). The comparison of Paleogene to older DZ distributions highlights the multiphase history of DZ recycling that is recorded in Cordilleran strata, ultimately showing that the presence of North American basement-aged grains in a sample does not necessarily reflect first-cycle derivation from North American basement terranes. Sediment provenance studies should acknowledge this limitation and should utilize additional information (such as paleogeographic, sedimentary facies, paleocurrent, or other types of provenance data) to inform interpretations of DZ distributions.

Acknowledgments
All new data presented herein for the Paleogene basin network (Renova Formation and equivalents) of southwestern Montana are publicly available online (https://www.geochron.org/dataset/html/geochron_dataset_2019_11_27_1ekDT). We gratefully acknowledge the authors of all previous detrital geochronology studies whose work facilitated the completion of this manuscript. Financial support for field work and new analyses was provided by Allegheny College through the William Howard Parsons Geology Endowment Fund, the John R. McClune Charitable Trust, the Cristine Scott Nelson Faculty Support Fund, and the Shanbrom Fund. We thank Chris Holm-Denoma, Paul Link, Kathy Surpless, and Susan Vuke for constructive reviews of this manuscript. Editor John Geissman and Associate Editor Cornelia Spiegel also provided constructive comments. Any use of trade, firm, or product names is for descriptive purposes only and does not imply endorsement by the U.S. Government.

References

Baar, E. E. (2009). Determining the regional-scale detrital zircon provenance of the Middle-Late Ordovician Kinnikinic (Eureka) Quartzite, east-central Idaho, U.S. [MS thesis]. Pullman WA: Washington State University, 134 p.

Beranek, L. P., Link, P. K., & Fanning, C. M. (2016). Detrital zircon record of mid-Paleozoic convergent margin activity in the northern U.S. Rocky Mountains: Implications for the Antler orogeny and early evolution of the North American Cordillera. *Lithosphere*, *8*, 533–550.

Blum, M., & Pecha, M. (2014). Mid-Cretaceous to Paleocene North American drainage reorganization from detrital zircons. *Geology*, *42*, 607–610. https://doi.org/10.1130/G35513.1

Bond, G. C., Christie-Blick, N., Kominz, M. A., & Devlin, W. J. (1985). An Early Cambrian rift to post-rift transition in the Cordillera of western North America. *Nature*, *316*, 742–745.

Carrapa, B., DeCelles, P. G., & Romero, M. (2019). Early inception of the Laramide orogeny in southwestern Montana and northern Wyoming: Implications for models of flat-slab subduction. *Journal of Geophysical Research: Solid Earth*, *124*, 2102–2123. https://doi.org/10.1029/2018JB016888

Cawood, P. A., Hawkesworth, C. J., & Dhuime, B. (2012). Detrital zircon record and tectonic setting. *Geology*, *40*, 875–878. https://doi.org/10.1130/G32945.1

Chapman, A. D., & Laskowski, A. K. (2019). Detrital zircon U-Pb data reveal a Mississippian sediment dispersal network originating in the Appalachian orogen, traversing North America along its southern shelf, and reaching as far as the southwest United States. *Lithosphere*, *11*, 581–587. https://doi.org/10.1130/L1068.1

Chetel, L. M., Janecke, S. U., Carroll, A. R., Beard, B. L., Johnson, C. M., & Singer, B. S. (2011). Paleogeographic reconstruction of the Eocene Idaho River, North American Cordillera. *GSA Bulletin*, *123*, 71–78.

Coney, P. J., & Harms, T. A. (1984). Cordilleran metamorphic core complexes: Cenozoic extensional relics of Mesozoic compression. *Geology*, *12*, 550–554.

Constenius, K. N. (1996). Late Paleogene extensional collapse of the Cordilleran foreland fold and thrust belt. *GSA Bulletin*, *108*, 20–39.

Cressman, E. R., & Swanson, R. W. (1964). Stratigraphy and petrology of the Permian rocks of southwestern Montana. U.S. Geological Survey Professional Paper 313-C, 569 p.

DeCelles, P. G. (1986). Sedimentation in a tectonically partitioned, nonmarine foreland basin: The Lower Cretaceous Kootenai Formation, southwestern Montana. *GSA Bulletin*, *97*, 911–931.

DeCelles, P. G. (2004). Late Jurassic to Eocene evolution of the Cordilleran thrust belt and foreland basin system, western U.S.A. *American Journal of Science*, *304*, 105–168.
Dickinson, W. R., Beard, L. S., Brakenridge, G. R., Erjavec, J. L., Fergusen, R. C., Inman, K. F., et al. (1983). Provenance of North American Phanerozoic sandstones in relation to tectonic setting. *GSA Bulletin*, *94*, 222–235.
Dumitru, T. A., Ernst, W. G., Wright, J. E., Wooden, J. L., Wells, R. E., Farmer, L. P., et al. (2013). Eocene extension in Idaho generated massive sediment floods into the Franciscan trench and into the Tyee, Great Valley, and Green River basins. *Geology*, *41*, 187–190.
Fields, R. W., Rasmussen, D. L., Tabrum, A. R., & Nichols, R. (1985). Cenozoic rocks of the intermontane basins of western Montana and eastern Idaho; a summary. In R. M. Flores, & S. S. Kaplan (Eds.), *Cenozoic paleogeography of the west-central United States: Rocky Mountain Section*, *Society of Economic Paleontologists and Mineralogists, Paleogeography Symposium* (Vol. 3, pp. 9–36). Denver, CO: The Rocky Mountain Section Society of Economic Paleontologists and Mineralogists.
Fildani, A., Hessler, A. M., Mason, C. C., McKay, M. P., & Stockli, D. F. (2018). Late Pleistocene glacial transitions in North America altered major river drainages, as revealed by deep-sea sediment. *Nature Scientific Reports*, *8*.
Fritz, W. J., Sears, J. W., McDowell, R. J., & Wampler, J. M. (2007). Cenozoic volcanic rocks of southwestern Montana. *Northwest Geology*, *36*, 91–110.
Fuentes, F., DeCelles, P. G., Constenius, K. N., & Gehrels, G. E. (2011). Evolution of the Cordilleran foreland basin system in northwestern Montana, U.S.A. *GSA Bulletin*, *123*, 507–533.
Fuentes, F., DeCelles, P. G., & Gehrels, G. E. (2009). Jurassic onset of foreland basin deposition in northwestern Montana, USA: Implications for along-strike synchroneity of Cordilleran orogenic activity. *Geology*, *37*, 379–382.
Gaschnig, R. M., Vervoort, J. D., Lewis, R. S., & McClelland, W. C. (2010). Migrating magmatism in the northern US Cordillera: In situ U-Pb geochronology of the Idaho batholith. *Contributions to Mineralogy and Petrology, v.*, *159*, 863–883.
Gehrels, G. E., Blakey, R., Karlstrom, K. E., Timmons, J. M., Dickinson, W. R., & Pecha, M. (2011). Detrital zircon U-Pb geochronology of Paleozoic strata in the Grand Canyon, Arizona. *Lithosphere*, *3*, 183–200.
Gehrels, G. E., & Pecha, M. (2014). Detrital zircon U-Pb geochronology and Hf isotope geochemistry of Paleozoic and Triassic passive margin strata of western North America. *Geosphere*, *10*, 49–65.
Graham, S. A., & Suttner, L. J. (1974). Occurrence of Cambrian islands in southwestern Montana. *The Mountain Geologist*, *11*, 71–84.
Haley, J. C., & Perry, W. J. (1991). The Red Butte Conglomerate—A thrust-belt-derived conglomerate of the Beaverhead Group, south-western Montana. *U.S. Geological Survey Bulletin* 1945, 19 p.
Houston, R. A., & Dilles, J. H. (2013). Structural geologic evolution of the Butte District, Montana. *Economic Geology*, *108*, 1397–1424.
Ingersoll, R. V., Kretchmer, A. G., & Valles, P. K. (1993). The effect of sampling scale on actualistic sandstone petrofacies. *Sedimentology*, *40*, 937–953.
Janecke, S. U., McIntosh, W., & Good, S. (1999). Testing models of rift basins: structure and stratigraphy of an Eocene-Oligocene supra-detachment basin, Muddy Creek half graben, south-west Montana. *Basin Research*, *11*, 143–165.
Laskowski, A. K., DeCelles, P. G., & Gehrels, G. E. (2013). Detrital zircon geochronology of Cordilleran retroarc foreland basin strata, western North America. *Tectonics*, *32*, 1027–1048. https://doi.org/10.1002/tect.20065
Leier, A. L., & Gehrels, G. E. (2011). Continental-scale detrital zircon provenance signatures in Lower Cretaceous strata, western North America. *Geology*, *39*, 399–402.
Link, P. K., Autenrieth-Durk, K. M., Cameron, A., Fanning, C. M., Vogl, J. J., & Foster, D. A. (2017). U-Pb zircon ages of the Wildhorse Gneiss, Pioneer Mountains, south-central Idaho, and tectonic implications. *Geosphere*, *13*, 681–698.
Link, P. K., Fanning, C. M., & Beranek, L. P. (2005). Reliability and longitudinal change of detrital-zircon age spectra in the Snake River system, Idaho and Wyoming: An example of reproducing the bumpy barcode. *Sedimentary Geology*, *182*, 101–142.
Link, P. K., Fanning, C. M., Lund, K. I., & Aleinikoff, J. N. (2007). Detrital-zircon populations and provenance of Mesoproterozoic strata of east-central Idaho, U.S.A.: Correlation with Belt Supergroup of southwest Montana. SEPM Special Publication No. 86, p. 101-128.
Link, P.K., Fanning, C.M., and Stroup, C.N. (2008) Detrital zircon U-Pb geochronologic data for selected Cretaceous, Paleogene, Neogene, and Holocene sandstones and river sands in southwest Montana and east-central Idaho. *Montana Bureau of Mines and Geology Open-File Report* 569, 5 p.
Link, P.K., Mahon, R.C., Beranek, L.P., Campbell-Stone, E.A., and Lynds, R. (2014) Detrital zircon provenance of Pennsylvanian to Permian sandstones from the Wyoming Craton and Wood River Bain, Idaho, U.S.A. *Rocky Mountain Geology*, v. 49, p. 115-136.
Link, P. K., Stewart, E. D., Steel, T., Sherwin, J., Hess, L. T., & McDonald, C. (2016). Detrital zircons in the Mesoproterozoic upper Belt Supergroup in the Pioneer, Beaverhead, and Lemhi Ranges, Montana and Idaho: The Big White arc. In J. S. MacLean, & J. W. Sears (Eds.), *Belt Basin: Window to Mesoproterozoic Earth*, *Geological Society of America Special Paper*, (Vol. 522, pp. 163–183). Boulder, CO.
Malone, D. J., Craddock, J. P., & Kenderes, S. (2017). Detrital zircon geochronology and provenance of the Middle Cambrian Flathead Sandstone, Park County, Wyoming. *The Mountain Geologist*, *54*, 86–103.
Maughan, E. K. (1990). Summary of the Ancestral Rocky Mountains epeirogeny in Wyoming and adjacent areas. *U.S. Geological Survey Open-File Report* OF 90-447, 8 p.
May, S. R., Gray, G. G., Summa, L. L., Stewart, N. R., Gehrels, G. E., & Pecha, M. E. (2013). Detrital zircon geochronology from the Bighorn Basin, Wyoming, USA: Implications for tectonostratigraphic evolution and paleogeography. *GSA Bulletin*, *125*, 1403–1422.
McLane, M. J. (1971). Phanerozoic detrital rocks at the north end of the Tobacco Root Mountains, southwestern Montana [PhD thesis]. Bloomington, IN: Indiana University, 253 p.
McLane, M. J. (1972). Sandstone: Secular trends in lithology in southwestern Montana. *Science*, *178*, 502–504.
McMannis, W. J. (1963). LaHood Formation—A coarse facies of the Belt Series in southwestern Montana. *GSA Bulletin*, *74*, 407–436.
Meyers, J. H., & Schwartz, R. K. (1994). Summary of depositional environments, paleogeography, and structural control on sedimentation in the Late Jurassic (Oxfordian) Sundance foreland basin, western Montana. In M. V. Caputo, J. A. Peterson, & K. J. Franczyk (Eds.), *Mesozoic systems of the Rocky Mountain Region, USA: The Rocky Mountain Section SEPM*, (pp. 331–350). Denver, CO: The Rocky Mountain Section Society of Economic Paleontologists and Mineralogists.
Mueller, P., Mogk, D., Wooden, J., & Spake, D. (2016). U-Pb ages from the Lower Belt Supergroup and proximal crystalline basement: Implications for the early evolution of the Belt Basin. In J. S. MacLean, & J. W. Sears (Eds.), *Belt Basin: Window to Mesoproterozoic Earth*, *Geological Society of America Special Paper*, (Vol. 522, chap. 11, pp. 283–304). Boulder, CO.
Perry, W. J. Jr., Haley, J. C., Nichols, D. J., Hammons, P. M., & Ponton, J. D. (1988). Interactions of Rocky Mountain foreland and Cordilleran thrust belt in Lima region, southwest Montana. In C. J. Schmidt, & W. J. Perry, Jr. (Eds.), *Interaction of the Rocky Mountain Foreland and Cordilleran Thrust Belt*, *GSA Memoir*, (Vol. 171, pp. 267–290). Boulder, CO.
Peters, S. E., & Gaines, R. R. (2012). Formation of the 'Great Unconformity' as a trigger for the Cambrian explosion. *Nature*, *484*(7394), 363–366. https://doi.org/10.1038/nature10969

Pullen, A., Ibanez-Mejia, M., Gehrels, G. E., Ibanez-Mejia, J. C., & Pecha, M. (2014). What happens when n = 1000? Creating large-n geochronological datasets with LA-ICP-MS for geologic investigations. *Journal of Analytical Atomic Spectrometry*, *28*, 971–980.

Quinn, G. M., Hubbard, S. M., Putnam, P. E., Matthews, W. A., Daniels, B. G., & Guest, B. (2018). A Late Jurassic to Early Cretaceous record of orogenic wedge evolution in the Western Interior basin, USA and Canada. *Geosphere*, *14*, 1187–1206.

Reynolds, M. W. (1979). Character and extent of Basin and Range faulting, western Montana and east-central Idaho. In G. W. Newman, & H. D. Goode (Eds.), *Basin and Range Symposium and Great Basin Field Conference: Denver, CO, Rocky Mountain Association of Geology and Utah Geological Survey*, (pp. 185–193). Denver, CO.

Romans, B. W., Castelltort, S., Covault, J. A., Fildani, A., & Walsh, J. P. (2016). Environmental signal propagation in sedimentary systems across timescales. *Earth-Science Reviews*, *153*, 7–29.

Ross, G. M., & Villeneuve, M. (2003). Provenance of the Mesoproterozoic (1.45 Ga) Belt basin (western North America): Another piece in the pre-Rodinia paleogeographic puzzle. *GSA Bulletin*, *115*, 1191–1217.

Saylor, J. E., Sundell, K. E., & Sharman, G. R. (2019). Characterizing sediment sources by non-negative matrix factorization of geochronological data. *Earth and Planetary Science Letters*, *512*, 46–58.

Scarberry, K. C., & Yakoklev, P. V. (2018). An overview of Mesozoic magmatism in Montana. In K. C. Scarberry, & S. Barth (Eds.), *Proceedings, Montana Mining and Mineral Symposium 2018 Technical Papers and Abstracts*, *Montana Bureau of Mines and Geology Special Publication*, (Vol. 120, pp. 57–62). Butte, MT.

Schwartz, R. K., & DeCelles, P. G. (1988). Foreland basin evolution and synorogenic sedimentation in response to interactive Cretaceous thrusting and reactivated foreland partitioning. In C. J. Schmidt, & W. J. Perry (Eds.), *Interaction of the Rocky Mountain Foreland and the Cordilleran Thrust Belt: GSA Memoir*, (Vol. 171, pp. 489–513). Boulder, CO.

Schwartz, R. K., O'Brien, T., Barber, D. E., Ness, J., & Weislogel, A. L. (2011). Braided channel system in the Paleogene Beaverhead intermontane basin: A longitudinal segment in the Paleo-Missouri headwater system of southwest Montana–detrital zircon age and provenance. *GSA Abstracts with Programs*, *43*(5), 431. www.researchgate.net/publication/334973710, https://doi.org/10.13140/RG.2.2.28800.79363

Schwartz, T. M., & Graham, S. A. (2017). Depositional history and provenance of Paleogene strata in the Sage Creek basin, southwestern Montana. *Geosphere*, *13*(4), 1285–1309. https://doi.org/10.1130/GES01450.1

Schwartz, T. M., Methner, K., Mulch, A., Graham, S. A., & Chamberlain, C. P. (2019). Paleogene topographic and climatic evolution of the Northern Rocky Mountains from integrated sedimentary and isotopic data. *GSA Bulletin*, *131*, 1203–1223. https://doi.org/10.1130/B32068.1

Schwartz, T. M., & Schwartz, R. K. (2013). Paleogene post-compressional intermontane basin evolution along the frontal Cordilleran fold-and-thrust belt of southwestern Montana. *GSA Bulletin*, *125*, 961–984.

Sears, J. W. (2013). Late Oligocene-early Miocene Grand Canyon: A Canadian connection? *GSA Today*, *23*, 4–10.

Sears, J. W., Link, P. K., Balgord, E. A., & Mahoney, J. B. (2010). Quartzite of Argenta, Beaverhead County, Montana, revisited: Definitive evidence of Precambrian age indicates edge of Belt Basin. *Northwest Geology*, *39*, 41–48.

Sears, J. W., & Ryan, P. C. (2003). Cenozoic evolution of the Montana Cordillera: Evidence from paleovalleys. In R. G. Raynolds, & R. M. Flores (Eds.), *Cenozoic systems of the Rocky Mountain Region*, *Denver, CO, Rocky Mountain Section, Society for Sedimentary Geology (SEPM)*, (pp. 289–299). Denver, CO.

Sharman, G. R., Covault, J. A., Stockli, D. F., Wroblewski, A. F. J., & Bush, M. A. (2016). Early Cenozoic drainage reorganization of the United States Western Interior-Gulf of Mexico sediment routing system. *Geology*, *45*(2), 187–190. https://doi.org/10.1130/G38765.1

Sharman, G. R., Graham, S. A., Grove, M., Kimbrough, D. L., & Wright, J. E. (2014). Detrital zircon provenance of the Late Cretaceous-Eocene California forearc: Influence of Laramide low-angle subduction on sediment dispersal and paleogeography. *GSA Bulletin*, *127*(1-2), 38–60. https://doi.org/10.1130/B31065.1

Sharman, G. R., & Johnstone, S. A. (2017). Sediment unmixing using detrital geochronology. *Earth and Planetary Science Letters*, *477*, 183–194.

Sharman, G. R., Sharman, J. P., & Sylvester, Z. (2018). detritalPy: A Python-based toolset for visualizing and analyzing detrital geo-thermochronologic data. *The Depositional Record*, *4*, 202–215.

Sloss, L. L. (1963). Sequences in the cratonic interior of North America. *GSA Bulletin*, *74*, 93–114.

Stewart, E. D., Link, P. K., Fanning, C. M., Frost, C. D., & McCurry, M. (2010). Paleogeographic implications of non-North American sediment in the Mesoproterozoic upper Belt Supergroup and Lemhi Group, Idaho and Montana. *Geology*, *38*, 927–930.

Stroup, C. N., Link, P. K., Janecke, S. U., Fanning, C. M., Yaxley, G. M., & Beranek, L. P. (2008). Eocene to Oligocene provenance and drainage in extensional basins of southwest Montana and east-central Idaho: Evidence from detrital zircon populations in the Renova Formation and equivalent strata. In J. E. Spencer, & S. R. Titley (Eds.), *Ores and orogenesis: Circum-Pacific Tectonics, geologic evolution, and ore deposits*, *Arizona Geological Society Digest*, (Vol. 22, pp. 529–546). Tucson, AZ.

Sundell, K. E., & Saylor, J. E. (2017). Unmixing detrital geochronology age distributions. *Geochemistry, Geophysics, Geosystems*, *18*, 2872–2886. https://doi.org/10.1002/2016GC006774

Vermeesch, P. (2013). Multi-sample comparison of detrital age distributions. *Chemical Geology*, *341*, 140–146.

Vermeesch, P., & Garzanti, E. (2015). Making geological sense of 'big data' in sedimentary provenance analysis. *Chemical Geology*, *409*, 20–27.

Vuke, S. M., Porter, K. W., Lonn, J. D., & Lopez, D. A. (2009). Geologic map of Montana field notebook: Montana Bureau of Mines and Geology Geologic Map 62E, scale 1:500,000.

Whitmeyer, S. J., & Karlstrom, K. E. (2007). Tectonic model for the Proterozoic growth of North America. *Geosphere*, *3*, 220–259.

Yonkee, W. A., Dehler, C. D., Link, P. K., Balgord, E. A., Keeley, J. A., Hayes, D. S., et al. (2014). Tectono-stratigraphic framework of Neoproterozoic to Cambrian strata, west-central U.S.: Protracted rifting, glaciation, and evolution of the North American Cordilleran margin. *Earth-Science Reviews*, *136*, 59–95.

Yonkee, W. A., & Weil, A. B. (2015). Tectonic evolution of the Sevier and Laramide belts within the North American Cordillera orogenic system. *Earth-Science Reviews*, *150*, 531–593.